On the assessment of multiaxial fatigue damage under variable amplitude loading

V. Anes, L. Reis, M. de Freitas
IDMEC, Instituto Superior Técnico, Universidade de Lisboa, Av. Rovisco Pais, 1049-001 Lisboa, Portugal.
vitor.anes@tecnico.ulisboa.pt, http://orcid.org/0000-0002-8526-398X
luis.g.reis@tecnico.ulisboa.pt, http://orcid.org/0000-0001-9848-9569
manuel.freitas@tecnico.ulisboa.pt, http://orcid.org/0000-0003-3525-9218

ABSTRACT. In this work, the performance of the SSF criterion is evaluated under variable amplitude loading conditions. The main objective was to inspect the validity of the hypothesis in which the SSF damage map remains valid for any high strength steel. In order to achieve that, fatigue life correlation of the 1050QT steel and 304L stainless steel was analyzed under multiaxial loading conditions. The loading block considered in the study comprises 360 proportional loading cycles with different stress amplitude ratios and stress levels. Despite being made of proportional branches, this loading block is a non-proportional loading due to its principal directions variation. This feature allows the evaluation of combined loading effects under variable amplitude loading conditions, which makes this loading block suitable to mimic the loading effects usually found in the field. Results show very good agreements, which reinforces the aforementioned hypothesis.

KEYWORDS. Multiaxial fatigue; Variable amplitude loading; Multiaxial cycle counting method; Fatigue life; Damage accumulation.

INTRODUCTION

In the field, random loadings are the most common type of load that we can find; typical examples can be found in car suspensions, aircraft wings or wind towers. This type of loadings is complex and difficult to deal with, specially their simulation in the lab. Also, their stochastic behavior increases the variability usually found in fatigue life experiments, which increases the complexity in damage accumulation assessment. They may have several loading effects that are usually studied separately in literature, however their combined effect can be activated simultaneously or sequentially under random loading conditions [1, 2]. Loading effects such as proportionality, non-proportionality, cyclic hardening, cyclic softening, mean stress, sequential and asynchronous loading, among others effects, cause different well known damage mechanisms [3-7], but their combined effect remains more or less unknown. Nowadays, there is a lack of knowledge in this matter and further research is required. This subject becomes extremely important when the assessment of instantaneous damage accumulation is required, such as in structural health monitoring procedures. Currently, the assessment of fatigue damage is not only performed in mechanical design stages, but also in structural integrity evaluation performed in the field. For example, damage accumulation tools can support on-condition maintenance decisions in order to optimize inspections and replacement costs. In the lab, the most common approach to simulate random loadings is to load pre-defined loading blocks in a randomly way. Thus, multiaxial fatigue models must be able to evaluate fatigue damage from variable amplitude loadings such as the ones found in multiaxial loading blocks. In this work, the present authors study the capability of the SSF criterion to capture fatigue damage under variable amplitude loading, which is a

fundamental prerequisite to estimate fatigue damage under random loading conditions. The main focus was on the hypothesis that states the existence of a typical SSF damage map for each material family.

THEORY, MATERIALS AND METHODOLOGY

Based on experiments the present authors have found out that fatigue damage from normal stresses have a damage scale different from the one found in shear stresses, especially under multiaxial loading conditions. Therefore, to compute a multiaxial damage parameter, both normal and shear stresses must be reduced to the same damage scale. In literature, this reduction is commonly performed using a constant; usually this constant is a function of uniaxial fatigue limits. However, results show that the damage scale between normal and shear stresses depends on the stress amplitude ratio λ, and also on the stress level [8]. To account these findings in fatigue damage assessment, the present authors developed the SSF equivalent shear stress. This damage parameter is an equivalent shear stress, were its magnitude represents the fatigue damage of a given multiaxial loading. Eq. (1) shows the SSF model; in the left the SSF equivalent shear stress and at right the uniaxial shear SN curve [8].

$$\max_{block}\left(\tau + ssf\left(\sigma_a,\lambda\right)\cdot\sigma\right) = A\left(N_f\right)^b \tag{1}$$

The $ssf\left(\sigma_a,\lambda\right)$ function shown in Eq. (1) is given in Eq. (2), this function is the so-called SSF damage map and aims to update the damage scale of normal stresses to the shear damage scale.

$$ssf\left(\sigma_a,\lambda\right) = a + b\cdot\sigma_a + c\cdot\sigma_a^{\,2} + d\cdot\sigma_a^{\,3} + f\cdot\lambda^2 + g\cdot\lambda^3 + h\cdot\lambda^4 + i\cdot\lambda^5 \tag{2}$$

where σ_a is the normal stress component of a given biaxial loading and λ is the stress amplitude ratio ($\lambda = \tau_a/\sigma_a$). The polynomial constants "a" to "i" are determined through experiments. The values of these constants for the 42CrMo4 steel are the following:

a=2.69; b=−9.90E−03; c=1.69E−05; d=−9.52E−09; f=−5.99; g=11.72; h=−8.04; i=1.63

Generalization of the SSF damage map

The SSF damage map, given by the 5th polynomial function shown in Eq. (2) was obtained for the 42CrMo4 material and translates its cyclic behavior under different stress amplitude ratios and stress levels. Therefore, the SSF fatigue estimates for other materials must be done using their SSF damage maps, which must be previously obtained by experiments. However, within a given steel family it has been assumed that the SSF damage map does not vary significantly, thus the SSF damage map computed for a given material of this family can be used as a typical SSF damage map and can be shared between material of this family. This assumption has been tested with success in two high strength steels, the Ck45 and C40, and is tested here with the 1050QT and 304L steels. The 1050QT clearly belongs to the 42CrMo4 family because their mechanical properties are very alike; please see Tab. 1. However, the mechanical properties of the 304L stainless steel are clearly out of the high strength steels family [9], thus it is expected a lower performance in the SSF fatigue life correlations for this material. The use of the 42CrMo4 SSF damage map in other materials is not performed directly, in these cases the SSF damage map must be updated using the tensile ultimate stresses as shown in Eq. (3).

$$\tau_{eq} = \tau + \left(\frac{\sigma_u}{\sigma_{u,42CrMo4}}\right)\cdot ssf(\sigma,\lambda)\cdot\sigma \tag{3}$$

where $\sigma_u/\sigma_{u,42CrMo4}$ is the ratio between the material's ultimate tensile stress (material that belongs to the 42CrMo4 family but its SSF damage map is unknown) and the ultimate tensile stress of the 42CrMo4 steel. The ultimate stress is a mechanical parameter that indicates clearly the steel family and has been used to estimate SN curves. Thus being the SSF damage map obtained based on the material SN curves under different stress amplitude ratios the use of the ultimate stress to perform this update was hypothesized and presented in [9].

Multiaxial cycle counting

Constant amplitude loadings are well characterized by its maximum damage parameter found within the loading pattern. However, in cases of variable amplitude loadings the maximum value of a given damage parameter do not captures the overall damage. In order to overcome this drawback, the present authors developed the virtual cycle counting method, which is a non-Rainflow cycle counting method for multiaxial loading conditions [10]. The virtual cycle counting (vcc) is based on the time evolution of the SSF equivalent shear stress and is given through Eq. (4).

$$vcc = \frac{\sum abs\left(\tau_{ssf}\right)_{peak,valley}}{2\cdot\tau_{\mathrm{ssf,max},Block}} \tag{4}$$

Where vcc can be understood as a virtual loading cycles calculation. In order to estimate the fatigue life of a given loading block using the SSF criterion, it is necessary to divide the fatigue life estimate, obtained with the maximum SSF equivalent stress found within the loading block, by the virtual cycle counting yield by Eq. (4).

Multiaxial loading path

Fig. 1 depicts the normal and shear stress time evolution of the loading path studied here, as well as, its representation on the von Mises stress space. This loading path is a non-proportional loading block made of 360 proportional loading paths loaded sequentially with a 1° degree gap between them.

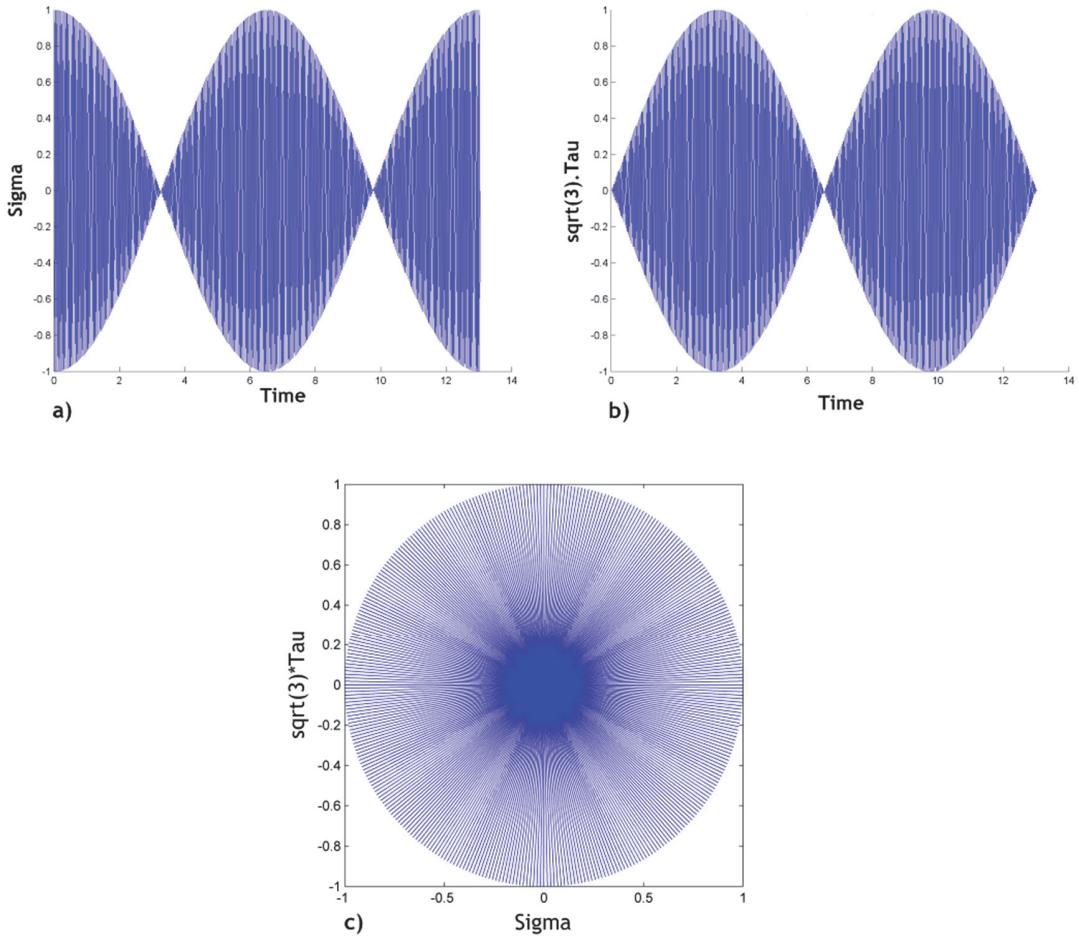

Figure 1: FRI loading path [11, 12]: a) normal stress time evolution, b) shear stress time evolution c) loading path depicted in the von Mises stress space.

The loading sequence starts with a stress amplitude ratio equal to zero and evolves in the anticlockwise direction until reach again the starting position. This loading path was firstly described in [11] and is a variable amplitude loading that activates all loading planes with the same equivalent stress amplitude during the block loading, please see Fig. 1 c).

Materials

In this study two different materials were considered to analyze the performance of the SSF equivalent shear stress under variable amplitude loadings. They are the 1050QT high strength steel and the 304L stainless steel. The 1050QT steel is a quenched and tempered medium-carbon steel and is usually used in forged shafts and gears. The 304L stainless steel has its applications in chemical processing, pulp and paper mills and food industry. Tab. 1 shows the monotonic and cyclic properties of the 1050QT and 304L steels. In addition, in column 2, the 42CrMo4 mechanical properties are shown, the SSF damage map used in this study was obtained for this material. As one can see, the 42CrMo4 and 1050QT mechanical properties are very alike, this similarity suggests that the 42CrMo4 SSF damage map can be fairly used to estimate the 1050QT SSF damage map.

	42CrMo4	**1050QT**	**304L**
Young's modulus, E (GPa)	206	203	195
Yield strength, (MPa)	980	1009	208
Ultimate tensile strength, (MPa)	1100	1164	585
Fatigue strength coefficient, (MPa)	1154	1346	1287
Fatigue strength exponent	-0.061	-0.062	-0.145

Table 1: 42CrMo4, 1050 QT and 304L stainless steel mechanical properties [8, 11, 12].

Fatigue life

Tab. 2 shows the stress levels of normal and shear stresses and their inherent fatigue life for the 1050QT steel and the 304L stainless steel. The fatigue life is shown in number of loading reversals. These experiments were performed under strain control and the failure condition was 20% drop in the testing stress level [11].

1050QT			**304L**		
Sigma max [MPa]	Tau max [MPa]	2Nf	Sigma max [MPa]	Tau max [MPa]	2Nf
724	413	3240	459	271	3960
751	432	4536	461	262	4176
632	374	29520	391	224	20160
620	364	64800	362	210	38160

Table 2: 1050QT and 304L fatigue life experimental results [11].

RESULTS AND DISCUSSION

Fig. 2 a) shows the SSF equivalent shear stress time evolution for the FRI loading block. This example is for the 1050QT material and for the maximum values of normal and shear stresses equal to 724 MPa and 413 MPa, respectively. The SSF time evolution depicted in Fig. 2 a) has 360 fully reversed loading cycles with variable amplitude and lead to a fatigue life equal to 3240 reversals, (please see first row of Tab. 2).

As it can be seen in Eq. (1), the maximum value found in the SSF time evolution is used, as a first iteration, to estimate the block fatigue life (i.e., the number of block repetitions before failure). In the second iteration, the first block fatigue life estimate (shown in Eq. (5) as $N_{1\max}$) is updated with the virtual cycle counting computed for the FRI loading block using Eq. (4), please see Eq. (5).

$$N_{f\_block} = \frac{N_{f\max}}{vcc} \tag{5}$$

Thus, it is expected that the fatigue failure will occur at N_{f_block} block repetitions. Fig. 2 b) shows the SSF equivalent loading block (equivalent to the FRI loading block) with a constant amplitude loading equal to 638 MPa, the SSF equivalent loading block has 300 loading cycles instead of the 360 cycles found in the FRI loading block.

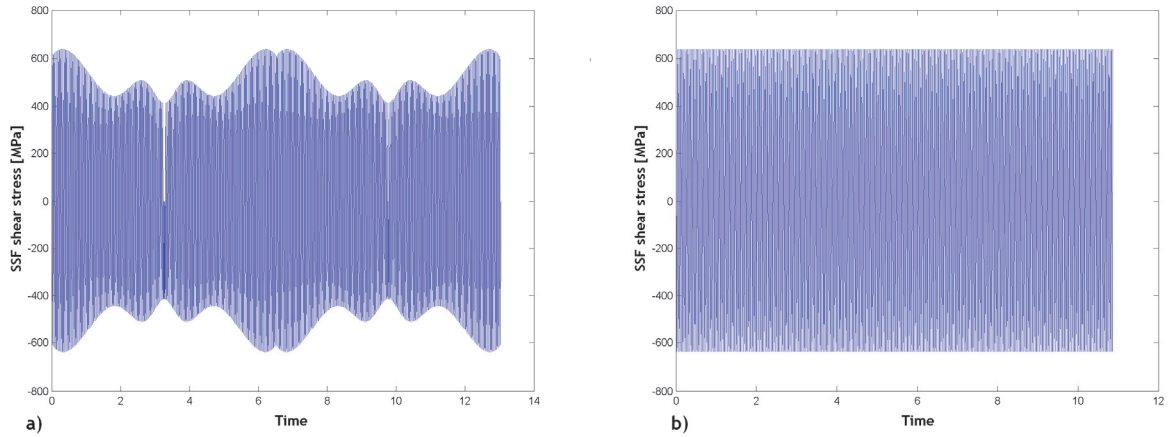

Figure 2: a) SSF equivalent stress time evolution for the FRI loading path (360 fully reversals), b) Constant amplitude SSF loading block (300 fully reversals).

Loading block results

Tabs. 3 and 4 show the results for the SSF fatigue life estimates, cycle counting, and number of block repetitions before failure. The experimental block results shown in the fourth column were obtained by dividing the number of experimental reversals at failure by 360 (360 proportional loadings found within the FRI loading block), this result shows the number of block repetitions during experiments at each stress level. The 5th column shows the SSF fatigue life estimates in number of reversal at failure time, these results were obtained using the material uniaxial shear SN curve. The 6th column shows the number of virtual loading cycles obtained with Eq. (4) for the FRI loading block.

The virtual cycle counting results in both materials were equal to 300 virtual loading cycles. Thus the fatigue damage of the 360 proportional loading cycles found in the FRI loading block is estimated by 300 virtual loading cycles with constant amplitude. This amplitude is given by the maximum SSF equivalent shear stress found within the loading block. Thus, the number of SSF loading blocks loaded before failure, shown in column 7, are obtained by dividing the number of loading cycles estimated by the SSF equivalent stress (shown in column 5 of Tabs. 3 and 4) and the number of virtual loading cycles computed for the FRI loading block.

Sigma max [MPa]	Tau max [MPa]	2Nf [11]	Exp blocks	SSF 2Nf	vcc	SSF blocks
724	413	3240	4,5	4617	300	8
751	432	4536	6,3	3070	300	5
632	374	29520	41	38718	300	65
620	364	64800	90	54587	300	91

Table 3: 1050QT loading block results.

Sigma max [MPa]	Tau max [MPa]	2Nf [11]	Exp blocks	ssf 2Nf	vcc	Ssf blocks
459	271	3960	5,5	2926	300	5
461	262	4176	5,8	3419	300	6
391	224	20160	28	7927	300	13
362	210	38160	53	11291	300	19

Table 4: 304L loading block results.

Thus, the FRI loading path (a variable amplitude loading) can be replaced by a constant amplitude loading using the SSF equivalent shear stress, and the virtual cycle counting method. This is particularly useful when one have loadings made of different loading blocks, which is may be the case of random loadings. Random loadings can be discretized into loading blocks [1] and treated as a damage accumulation case, however multiaxial criteria used in damage accumulation procedures must be able to capture fatigue damage of variable amplitude loadings.

Fig. 3 depicts the fatigue life correlation for the two materials considered in this study. These results show that the 42CrMo4 damage map is suitable for high strength steels, which confirms previous studies performed by the present authors [9]. These results are reinforced by the 1050QT correlation pattern where the correlation slope is parallel to the boundary lines - please see Fig. 3. On the other hand, the correlation slope of the 304L steel is quite different from the slope of the boundary lines, i.e. the correlation trend line of the 304L fatigue data crosses the lower boundary lines. This indicates that the damage map of the 42CrMo4 high strength steel do not capture in full the 304L fatigue pattern, which is a result expected by the present authors. Stainless steels are extremely sensitive to non-proportionality and show strong variation of their mechanical properties under cyclic loadings. Thus their cyclic behavior is quite different from the one that is usually found in high strength steels.

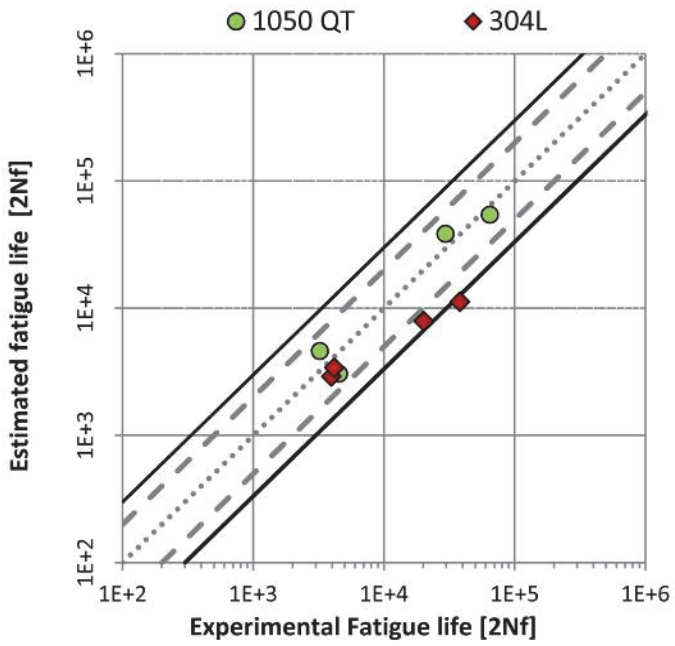

Figure 3: SSF fatigue life correlation for the 1050QT and 304L steels.

CONCLUSIONS

The present study evaluates the performance of the SSF criterion under variable amplitude loading for two different materials, i.e. the 1050QT steel and the 304L stainless steel. The idea was to inspect the validity of the 42CrMo4 SSF damage map for other materials under variable amplitude loading conditions. The present authors have been using the 42CrMo4 SSF damage map in fatigue life predictions of high strength steels with success; examples are the Ck45 and C40 steels. The main focus of the SSF criterion has been on the idea that the damage scale of normal and shear stresses of a given multiaxial loading is not constant. This damage scale is strongly dependent on the stress level and stress amplitude ratio and can be evaluated with the so-called SSF damage map. In this paper, results confirm the validity of the 42CrMo4 SSF damage map for high strength steels, as seen in the obtained results for the 1050QT steel. This steel has mechanical properties very close to the 42CrMo4 properties, in some of them the 1050QT has higher values, thus it can be considered that both materials belong to the same steel family. Based on the results found here and based on previous results computed for the Ck45, and C40 high strength steels, it can be considered that a SSF damage map can be defined for each material family. To reinforce this, the results for the 304L stainless steel where not so good, which indicates the necessity to obtain the SSF damage map for this steel family.

ACKNOWLEDGEMENTS

This work was supported by FCT, through IDMEC, under LAETA project UID/EMS/50022/2013.

REFERENCES

[1] Anes, V., Reis, L., de Freitas, M., A new criterion for evaluating multiaxial fatigue damage under multiaxial random loading conditions, Advanced Materials Research, 181 (2014) 1360–1365. doi:10.4028/www.scientific.net/AMR.891-892.1360.

[2] Wang, Y., Susmel, L., The Modified Manson–Coffin Curve Method to estimate fatigue lifetime under complex constant and variable amplitude multiaxial fatigue loading, International Journal of Fatigue, 83 (2016) 135–49. doi:10.1016/j.ijfatigue.2015.10.005.

[3] Chaves, V., Navarro, A., Madrigal, C., Stage I crack directions under in-phase axial–torsion fatigue loading for AISI 304L stainless steel, International Journal of Fatigue, 80 (2015) 10–21. doi:10.1016/j.ijfatigue.2015.05.004.

[4] Chaves, V., Madrigal, C., Navarro, A., Biaxial fatigue tests and crack paths for AISI 304L stainless steel, Frattura ed Integritá Strutturale, 30 (2014) 273. doi: 10.3221/IGF-ESIS.30.34.

[5] Carpinteri, A., Ronchei, C., Spagnoli, A., Vantadori, S., Lifetime estimation in the low/medium-cycle regime using the Carpinteri–Spagnoli multiaxial fatigue criterion, Theoretical and Applied Fracture Mechanics, 73 (2014) 120–127. doi:10.1016/j.tafmec.2014.06.002.

[6] Carpinteri, A., Ronchei, C., Scorza, D., Vantadori, S., Critical Plane Orientation Influence on Multiaxial High-Cycle Fatigue Assessment, Physical Mesomechanics. 18 (2015) 348–54. doi:10.1134/S1029959915040074.

[7] Campagnolo, A., Berto, F., Marangon, C., Cyclic plasticity in three-dimensional notched components under in-phase multiaxial loading at R=- 1, Theoretical and Applied Fracture Mechanics, 81 (2016) 76–88. doi:10.1016/j.tafmec.2015.10.004.

[8] Anes, V., Reis, L., Li, B., Fonte, M., De Freitas, M., New approach for analysis of complex multiaxial loading paths, International Journal of Fatigue, 62 (2014) 21–33. doi:10.1016/j.ijfatigue.2013.05.004.

[9] Anes, V., Reis, L., Li, B., Freitas, M., Sonsino, C.M., Minimum Circumscribed Ellipse (MCE) and Stress Scale Factor (SSF) criteria for multiaxial fatigue life assessment, Theoretical and Applied Fracture Mechanics, 73 (2014) 109–19. doi:10.1016/j.tafmec.2014.08.008.

[10] Anes, V., Reis, L., Li, B., de Freitas, M., New cycle counting method for multiaxial fatigue, International Journal of Fatigue, 67 (2014) 78–94. doi:10.1016/j.ijfatigue.2014.02.010.

[11] Shamsaei, N., (2010). PhD Thesis, Univ. of Illinois at Urbana-Champaign, USA.

[12] Shamsaei, N., Fatemi, A., Socie, D.F., Multiaxial fatigue evaluation using discriminating strain paths, International Journal of Fatigue, 33 (2011) 597–609. doi:10.1016/j.ijfatigue.2010.11.002.